

# Influences of incoherent optical feedback on the nonlinear dynamical characteristics of an optically injected semiconductor laser

XIN-XIN PING<sup>a</sup>, XIAO-DONG LIN<sup>a</sup>, ZHENG-MAO WU<sup>a</sup>, LI WANG<sup>a</sup>, GUANG-QIONG XIA<sup>a,b,\*</sup>

<sup>a</sup>*School of Physics, Southwest University, Chongqing 400715, China*

<sup>b</sup>*Key Lab of Fiber Sensing and Communications, Ministry of National Education, University of Electronic Science and Technology of China, Chengdu 610054, China*

In this paper, the influences of incoherent optical feedback on the nonlinear dynamical characteristics of an optically injected semiconductor laser (SL) have been investigated numerically. Based on the bifurcation diagram of the extrema of peak series, it can be found that, after introducing incoherent optical feedback, the nonlinear dynamics of an optically injected SL will follow different routes to chaos oscillation. Period-doubling pulsing route and quasi-periodic pulsing route have been observed, which are different from that found in an optically injected SL without incoherence optical feedback. Mappings of dynamic states in the parameters space are plotted for different incoherence feedback strengths. Compared with an optically injected SL without incoherent optical feedback, a larger expansion of chaos region is observed.

(Received June 21, 2010; accepted August 12, 2010)

*Keywords:* Semiconductor laser (SL), Nonlinear dynamics, Optical injection, Incoherent optical feedback

## 1. Introduction

Nonlinear dynamics of semiconductor lasers (SLs) under external perturbation [1-20] have attracted much attention due to its potential applications such as cryptographic communications, optical memory, spectroscopy and other fields. Through introducing external perturbation such as optical injection [1-4], optical feedback [5-8] and optoelectronic feedback [9, 10], the output of a SL can exhibit various dynamical states and follow different routes to chaos. In the early research stage, one usually focused on the nonlinear dynamic of a SL subject to one perturbation. Recently, the dynamics characteristics of a SL subject to more than one perturbation have attracted more and more attention [11-20]. In Ref. [11, 12], an additional optical injection is introduced into an optically injected SL in order to enrich and control chaos. In Ref. [13], it has been demonstrated that tailored optoelectronic feedback can be selectively used to excite periodic dynamical output from external cavity semiconductor lasers. For an external cavity SL, the time delay signature can be suppressed efficiently through introducing another external cavity [14], and the bandwidth of chaotic output can be enhanced through introducing optical injection [15-19]. For an optically injected SL, after adopting optoelectronic feedback, a notable expansion and shifting of the chaos region in the parameter space was observed [20]. However, it is inevitable that the chaotic bandwidth will be limited by the low-pass filtering effect of electronic device used in this

system.

In this paper, incoherent optical feedback has been introduced into an optically injected SL, and the output dynamical characteristics of SL are investigated numerically. Due to all-optical components in this system, the bandwidth is not limited by electronic bandwidth. By adjusting the injection strength, the laser can follow two typical routes to chaos pulsing (CP), where one is period-doubling pulsing route to CP and the other is quasi-periodic pulsing route to CP. Furthermore, for different incoherent optical feedback strength, the map of dynamical states in the parameter space consisting of the injection strength and the frequency detuning has also been given. Compared with that an optically injected SL without incoherence optical feedback, the chaos region is enlarged and the dynamic states are greatly enriched.

## 2. Theoretical model

The dynamic of an optically injected SL subject to incoherence optical feedback can be modeled by the following rate equations:

$$\frac{dE}{dt} = \frac{1}{2} [G(N - N_0) - \frac{1}{\tau_p}] E + \frac{k_{inj}}{\tau_{in}} E_{inj} \cos \theta(t) \quad (1)$$

$$\frac{dN}{dt} = \frac{I}{eV} - \frac{N}{\tau_n} - G(N - N_0) |E|^2 - k_f G(N - N_0) |E(t - \tau)|^2 \quad (2)$$

$$\frac{d\phi}{dt} = \frac{1}{2} \alpha [G(N_2 - N_0) - \frac{1}{\tau_p} E_2 - \frac{k_{inj}}{\tau_{in}} \frac{E_{inj}}{E}] \sin \theta(t) \quad (3)$$

$$\theta(t) = \phi + \Delta v t \quad (4)$$

where  $E$  and  $\phi$  are the amplitude and phase of electric field, respectively,  $N$  is the carrier density,  $N_0$  is the carrier density at transparency,  $\alpha$  is line-width enhancement factor,

$V$  is the volume of active-region,  $G = \frac{g}{1 + \varepsilon |E|^2}$  ( $g$  is the

linear gain coefficient,  $\varepsilon$  is the gain saturation coefficient) is the optical gain coefficient,  $e$  is the electron charge,  $\tau_n$  is the carrier lifetime,  $\tau_p$  is the photon lifetime,  $\tau_{in}$  is the round-trip time of light in the laser cavity,  $I$  is the bias current.  $E_{inj}$  and  $\omega_{inj}$  are the amplitude and frequency of injection optical field, respectively.  $\Delta v = (\omega_{inj} - \omega) / 2\pi$  ( $\omega$  is the angular frequency of free-running SL, and  $\omega_{inj}$  is the frequency of injection optical field) is frequency detuning,  $\tau$  is the feedback delay time,  $k_{inj}$  and  $k_f$  are the injection and feedback strength, respectively.

The numerical results are calculated by using the following parameters values:  $\alpha=3$ ,  $V=1 \times 10^{-16} \text{ m}^3$ ,  $g=6.8 \times 10^{-13} \text{ m}^3/\text{s}$ ,  $e=1.6 \times 10^{-19} \text{ C}$ ,  $\tau_n=2.5 \text{ ns}$ ,  $\tau_p=3 \text{ ps}$ ,  $\tau_{in}=8 \text{ ps}$ ,  $N_0=1.25 \times 10^{24} / \text{m}^3$ ,  $E_{inj}=3.9342 \times 10^{10} \text{ m}^{-3/2}$ ,  $\tau=6 \text{ ns}$ ,  $\varepsilon=0$ ,  $I=1.5I_{th}$ , and the threshold current  $I_{th}=12.9 \text{ mA}$ . With above given parameters, the relaxation oscillation frequency of the free-running SL is 2.98 GHz and is estimated by  $f=1/[2\pi(gE^2/\tau_p)^{-1/2}]$  [13].

### 3. Results and discussion

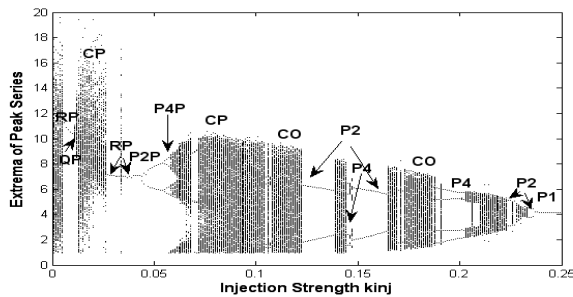


Fig. 1. Bifurcation diagrams of the extrema of the peak series for  $k_f = 0.184$  and  $\Delta v = 3.77 \text{ GHz}$ , where the injection strength  $k_{inj}$  varies from 0 to 0.25. The symbols are as follows: RP: regular pulsing; QP: quasi-periodic pulsing; P2P: two-frequency pulsing; P4P: four-frequency pulsing; CP: chaotic pulsing; P1: period-one; P2: period-two; P4: period-four; CO: chaotic oscillation.

Fig. 1 shows the extrema of the peak series plotted by increasing the injection strength  $k_{inj}$  from 0 to 0.25 for  $k_f = 0.184$ ,  $\Delta v = 3.77 \text{ GHz}$ . The optically injected SL with incoherence feedback can be operated at the regular pulsing (RP), quasi-periodic pulsing (QP), two-frequency pulsing (P2P), four-frequency pulsing (P4P), chaotic pulsing (CP), period-one (P1), period-two (P2), period-four (P4), chaotic oscillation (CO). From this diagram, it can be seen that there exists different routes to chaos, where two typical pulsing routes are observed. One is period-doubling pulsing route, which follows RP, P2P, P4P, to CP, and the other is quasi-periodic pulsing route, which follows RP, QP, to CP. These two routes are plotted in Fig. 2 and Fig. 3.

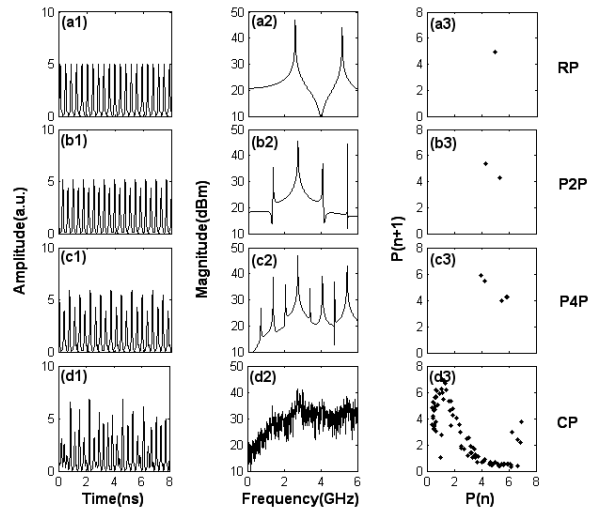


Fig. 2. Time series (left column), power spectra (middle column), and phase portrait (right column) of different states with  $k_f = 0.184$  and  $\Delta v = 3.77 \text{ GHz}$  for showing the period-doubling pulsing route to chaos, where  $k_{inj} = 0.04$ , 0.046, 0.056, and 0.08 corresponds to (a) RP, (b) P2P, (c) P4P and (d) CP state, respectively.

Fig. 2 shows the period-doubling pulsing route to CP by increasing the injection strength from 0.045 to 0.08, where the time series, the power spectra, and phase portrait are given. Fig. 2(a) shows the RP state, where the pulses with same intensity pulsing at the frequency of 2.583 GHz and a single dot in the phase portrait can be seen. As injection strength increased to 0.046, the output state is a P2P state as shown in Fig. 2(b). The pulses intensity has two distinctive values which repeat one after the other. Except the pulsing frequency  $f_1 = 2.725 \text{ GHz}$ , the sub-harmonic  $f_1/2$  also shows upon the power spectra, and two dots is observed in the phase portrait. Therefore, the output state is a P2P state. For  $k_{inj} = 0.056$  (see Fig. 2(c)), there are four distinctive values in the pulse intensity, four frequency components at  $f_1/4$ ,  $f_1/2$ ,  $3f_1/4$ ,  $f_1$  in the power spectra, and four distinctive spots in the phase portrait,

which are the characteristics of P4P state. For  $k_{inj}=0.08$  (see Fig. 2(d)), the pulse intensity varies chaotically, the power spectrum is broadened, and the phase portrait shows

a highly scattered distribution in a large area. So, the output is in a chaotic pulsing state under this circumstance.

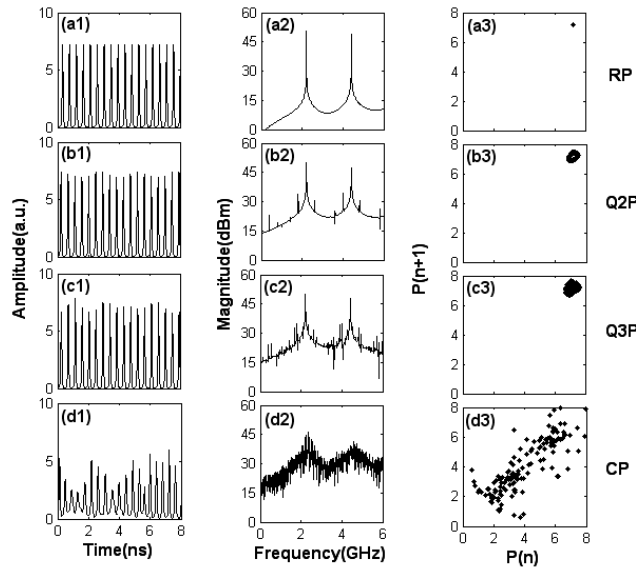


Fig. 3. Time series (left column), power spectra (middle column), and phase portrait (right column) of different states with  $k_f=0.184$ ,  $\Delta\nu=3.77$  GHz for showing the quasi-periodic pulsing route to chaos, where  $k_{inj}=0.01, 0.011, 0.0113$  and  $0.0123$  corresponds to RP (a), quasi-periodic two-frequency pulsing (Q2P) (b), quasi-periodic three-frequency pulsing (Q3P) (c) and CP (d), respectively.

Fig. 3 shows the quasi-periodic pulsing route to CP. The RP and CP state in Fig. 3 (a) and Fig. 3 (d) shows the same characteristics as the RP and CP shown in Fig. 2 (a) and Fig. 2 (d). For  $k_{inj}=0.011$  (see Fig. 3(b)), quasi-periodic two-frequency pulsing (Q2P) state can be observed, where a frequency of 405MHz that is incommensurate with the

pulsing frequency appears in the power spectrum. In the phase portrait for this state, a ring-like distribution is found. For  $k_{inj}=0.0113$  (see Fig. 3(c)), the laser will be driven into Q3P state. Compared with the Q2P state, an additional frequency 535MHz appears in the power spectrum and a torus is observed in phase portrait.

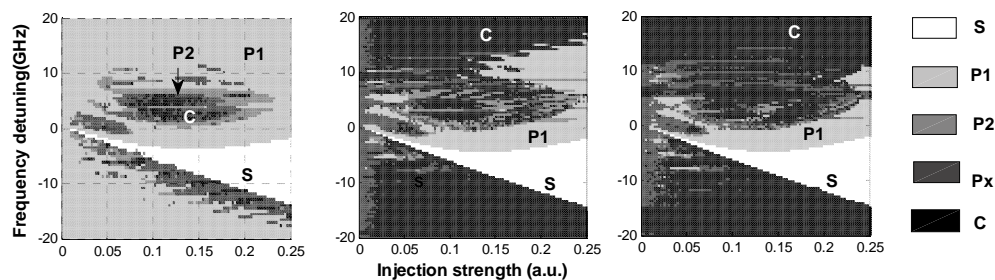


Fig. 4. Mappings of the dynamic state of an optically injected SL under incoherence optical feedback strengths  $k_f=0$ (left),  $0.12$ (middle),  $0.184$ (right). The symbols are as follows: S, stable locking; P1, period-one oscillation; P2, period-two oscillation; Px, unified presentation of other dynamics, e. g., period-four and quasi-periodic; C, chaos

.In order to reveal the influences of the incoherent feedback on an optically injected SL, Fig. 4 gives the map of dynamical states in the parameter space consisting of the relatively coupling level  $k_{inj}$  and the frequency detuning  $\Delta\nu$  under different incoherent feedback strength

$k_f$ . The white color corresponds to the stable locking (S) region, while P1, P2, period-four and quasi-periodic (Px), chaos states (C) are denoted by different grey scales as shown in the color bar. Fig. 4(a) is the map of dynamic state in an optically injected system without incoherence

optical feedback, where the chaos region (C) is small. With the increase of incoherent optical feedback strength, the significant expansion of the chaos regions is observed.

#### 4. Conclusions

After introducing incoherent optical feedback, the nonlinear dynamics characteristics of an optically injected SL have been studied numerically. Different dynamic states, including stable locking, regular pulsing, periodic pulsing, quasi-periodic pulsing and chaotic pulsing, are observed by varying the parameters of injection and feedback strength. Meantime, two typical routes to chaos, named as the period-doubling pulsing route and the quasi-periodic pulsing route, have been found. Furthermore, under different feedback strengths, the map of dynamic states in the parameter space has been given, and significant expansion of the chaos region is observed after introducing incoherent optical feedback.

#### Acknowledgements

This work was supported by the National Natural Science Foundation of China under Grant No. 60978003, the Fundamental Research Funds for the Central Universities under Grant No. XDJK2009B010, and the Open Fund of the Key Lab of Fiber sensing and communication, Ministry of Education, China.

#### References

- [1] T. B. Simpson, J. M. Liu, K. F. Huang, K. Tai, *Quantum Semiclass. Opt.* **9**, 765 (1997).
- [2] S. Wiczorek, T. B. Simpson, B. Krauskopf, D. Lenstra, *Opt. Commun.* **215**, 125 (2003).
- [3] T. B. Simpson, *Opt. Commun.* **215**, 135 (2003).
- [4] H. J. Kong, Z. M. Wu, J. G. Wu, Y. K. Xie, X. D. Lin, G. Q. Xia, *Chaos, Solitons and Fractals* **36**, 18 (2008).
- [5] S. Fukuchi, S. Y. Ye, J. Ohtsubo, *Opt. Rev.* **6**, 365 (1999).
- [6] J. Mork, B. Tromborg, J. Mark, *IEEE J. Quantum Electron.* **28**, 93 (1992).
- [7] J. M. Saucedo Soloria, D. W. Sukow, D. R. Hicks, A. Gavrielides, *Opt. Commun.* **214**, 327 (2002).
- [8] R. Ju, P. S. Spencer, *J. Lightwave Technol.* **23**, 2513 (2005).
- [9] F. Y. Lin, J. M. Liu, *IEEE J. Quantum Electron.* **39**, 562 (2003).
- [10] G. Q. Xia, S. C. Chan, J. M. Liu, *Opt. Express* **15**, 572 (2007).
- [11] J. Troger, L. Thevenaz, P. A. Nicati, P. A. Robert, *J. Lightwave Technol.* **17**, 629 (1999).
- [12] N. M. Al-honsiny, I. D. Henning, M. J. Adams, *Opt. Commun.* **269**, 166 (2006).
- [13] S. I. Turovets, J. Dellunde, K. A. Shore, *J. Opt. Soc. Am. B* **14**, 200 (1997).
- [14] J. G. Wu, G. Q. Xia, Z. M. Wu, *Opt. Express* **17**, 20124 (2009).
- [15] J. S. Lawrence, D. M. Kane, *Opt. Commun.* **167**, 273 (1999).
- [16] Y. Takiguchi, K. Ohyagi, J. Ohtsubo, *Opt. Lett.* **28**, 319 (2003).
- [17] A. B. Wang, Y. C. Wang, J. F. Wang, *Opt. Lett.* **34**, 1144 (2009).
- [18] X. D. Lin, G. Q. Xia, T. Deng, J. G. Chen, Z. M. Wu, *Optoelectron. Adv. Mat. – Rap. Commun.* **3**, 1129 (2009).
- [19] H. Someya, I. Oowada, H. Okumura, T. Kida, A. Uchida, *Opt. Express* **17**, 19536 (2009).
- [20] F. Y. Lin, J. M. Liu, *Opt. Commun.* **221**, 173 (2003).

\*Corresponding author: gqxia@swu.edu.cn